Spatial and Spatio-temporal Epidemiology 34 (2020) 100358

Contents lists available at ScienceDirect

Spatial and Spatio-temporal Epidemiology

journal homepage: www.elsevier.com/locate/sste

Exploring spatio-temporal patterns in mental health related emergency department use from children and adolescents

Michelle Thiessen[a,c], Qi Cui[a], X. Joan Hu[a], Rhonda J. Rosychuk[b,*]

[a] Department of Statistics and Actuarial Science, Simon Fraser University, Burnaby, British Columbia, Canada
[b] Department of Pediatrics, University of Alberta, Edmonton, Alberta, Canada
[c] Winnipeg, Manitoba, Canada

ARTICLE INFO

Article history:
Received 29 November 2019
Revised 15 June 2020
Accepted 18 June 2020
Available online 20 June 2020

Keywords:
Generalized linear model
Mixed effects
Regression analysis
Seasonal effect

ABSTRACT

To understand the spatio-temporal patterns and associated risk factors with the frequency, we analyze records of mental health related emergency department (MHED) visits from youth. The data are extracted for the period 2002–2011 from the population-based, provincial health administrative data systems of Alberta, Canada. Guided by a descriptive analysis, we conduct generalized linear regression analyses of the counts of MHED visits from various health areas. Seasonal effects are examined via three different types of functions, including trigonometric functions. We specify the temporal correlation using an autoregressive model of order 1 and formulate the spatial correlation by a random effects model. Our analysis reveals a strong seasonal pattern and indicates that the MHED visit counts are significantly associated with age, gender, and a proxy for socio-economic status. The final statistical model may be used to forecast future MHED use and identify regions and groups at a higher risk to the MHEDs.

1. Introduction

Mental health is a relatively understudied subject matter, yet it is estimated that 29% of Canadian youth aged 13–19 years are affected by mental health issues (Mental Health Commission of Canada, 2012). Unfortunately only 20% of those who need mental health services receive them (Leitch, 2007). There is a lack of community-based supports for mental health services, and inpatient and outpatient treatment options in Alberta, Canada. This often leads to families seeking for help at emergency departments during crises (Newton et al., 2011). Mental health related emergency department (MHED) visits can often be avoided if treatment is sought out before the crisis point is reached. Learning more about when and where the capacity of the pediatric mental health care system is exceeded by the need can help the province of Alberta understand where more resources are needed and reduce crowding in emergency departments. Potential policy implications partly motivated the research presented in this paper.

Researchers have previously examined geographical clustering of MHED visits. Mariathas and Rosychuk (2015) studied three different spatial cluster detection methods that differed in their choice of distributional assumption. Emergency department visits by children and youth aged less than 18 years old for substance use during April 1, 2007 to March 31, 2008 were used. Statistically significant clusters were found in northern Alberta, parts of the Edmonton region, and southwestern Alberta for all three detection methods. Rosychuk et al. (2014) used emergency department visits due to a mood disorder for Albertans aged 10–17. The Kulldorff-Nagarwalla (KN) spatial scan test (Kulldorff and Nagarwalla, 1995) found three potential clusters over space and time in the majority of northern Alberta between 2007 and 2011, in a single sub-regional health authority (sRHA) in the southwest part of the Central Zone between 2005 and 2009, and another in the Central Zone between 2008 and 2011. Rosychuk et al. (2016) used the KN spatial scan on Albertans aged 15–17 years during 2002–2011 who visited an emergency department for self-harm and had no physician follow-up visit within 14 days post-ED visit. They found a cluster in northern Alberta from 2002–2006 and in southern Alberta between 2003–2007.

Marginal regression models have also been used to examine MHED visits. Hu and Rosychuk (2016) and Rosychuk et al. (2018) investigate age-varying effects of risk factors on pediatric MHED visit frequencies by marginal regression analyses of the data. They show that older male subjects have lower MHED visit frequencies compared to females than younger males. Their studies assume that the MHEDs were generated from independent subjects. The MHED visits are in fact naturally clustered according to the associated health sub-regions in Alberta, and it is important to

* Corresponding author.
E-mail address: rhonda.rosychuk@ualberta.ca (R.J. Rosychuk).

https://doi.org/10.1016/j.sste.2020.100358
1877-5845/

know about the correlation. In addition, a good understanding of seasonal effects to MHED use is often desirable.

We aim to explore the spatio-temporal patterns in the MHED use and identify important risk factors associated with the frequency. The rest of this paper is organized as follows. Section 2 starts with a descriptive analysis of the PMHC dataset. The generalized linear mixed effects model for the final inferential analysis emerges from analyses of the data under various plausible regression models. Section 3 describes the model associated estimation procedure and presents the analysis results with the PMHC dataset. Final remarks and future work are given in Section 4.

2. PMHC dataset and statistical modelling

2.1. Alberta pediatric mental health (PMHC) dataset

The PMHC dataset used in this paper was taken from two population-based administrative databases in Alberta, the Ambulatory Care Classification System (ACCS) and the Population Registry File (PRF). The ACCS database provides Alberta MHED visit information. The demographic and geographic data are from the PRF database. The individuals of interest are Alberta residents who had at least one MHED visit and were younger than 18 years old at the time of their MHED visit during the observation window April 1, 2002 to March 31, 2011. An Alberta resident is defined as an individual who is registered in the Alberta Health Care Insurance Plan (AHCIP). Geographic location data are reported as the residence at fiscal year end and thus our calculations use fiscal years rather than calendar years.

In 2003, Alberta was divided into 9 regional health authorities (RHAs), and further divided into 70 sub-regional health authorities (sRHAs). Fig. 1 shows the choropleth maps of the number of MHED visits per 1000 sRHA population over 9 fiscal years. Five intervals were chosen based on Fisher-Jenks natural breaks algorithm (Jenks, 1977) as they provided a good spread of the rates of MHED visits and had both the highest goodness of variance fit measure and tabular accuracy index compared to other approaches considered. We can see that sRHAs in RHA 3 and RHA 6, the major urban areas of the Calgary and Edmonton area, respectively, are in the higher range of MHED visits per 1000 sRHA population. Interestingly, the sRHAs in RHA 9, the northern area of the province, is in the lower range of MHED visits in the early 2000s but has an increase in visit rates and is now in the higher range bracket for 2010/2011. These choropleth maps show that the rate of MHED visits is different not only across sRHAs, but over time as well.

Fig. 2 shows the monthly variation of MHED visits for the nine different RHAs. The RHAs appear to follow a similar seasonal pattern. They all have a decrease in MHED visits in the summer months, July and August, and increases in the winter months, October and November, as well as March and May. This motivates exploring a cyclic seasonal effect for the MHED visits.

The PMHC dataset has the following demographic information collected on the individuals. The individual's age at the time of the MHED visit and at fiscal year end, the proxy for socio-economic status (pSES), and gender. The age of the individual at fiscal year end means that some individuals who were aged 17 at the time of MHED visit might have turned 18 by the end of the fiscal year. The population data records the age at fiscal year end. In order to match the population data, the age at fiscal year end is chosen. The proxy for socio-economic status included three categories based on level of income support or source of payment for premium, denoted as $pSES_1$, $pSES_2$, and $pSES_3$.

Table 1 summarizes the number of MHED visits by demographic information with data taken from the ACCS and PRF databases. From Table 1, it can be seen that females, teenagers aged 13–18 at the fiscal year end and $pSES_1$ individuals comprise of the majority of MHED visits for all of the 9 fiscal years. The age groups 0–5 and 6–12 years old are combined in the analysis due to low counts of MHED visits.

2.2. Notation and model specifications

This paper focuses on the primary response $Y(t; r; \boldsymbol{x})$ to be the number of the MHED visits at time t and region r with covariates $\boldsymbol{x}$. Specifically, the region index r is $1, \ldots, 70$ for the 70 sRHAs. We use R to denote the RHAs, where $R = 1,\ldots,9$ for the 9 RHAs. The number of sRHAs within RHAs varies by RHA. We consider the time starting at April 1, 2002 and with the unit of a 28 day block. Thus each fiscal year has 13 time units (blocks) and $t = 1, \ldots, 117$ with the MHED data. The advantage of using 13 blocks over a monthly time unit is that each time unit has an equal amount of days. This ensures the variations in counts between blocks will not be due to differences in amount of days. Another method would have been to introduce an offset in the Poisson regression that adjusts for the unequal number of days in the months using (365.25/12)/(days in month t) (Barnett and Dobson, 2010).

Since the response variable is in the form of counts, we assume it follows a Poisson distribution conditional on its covariates. The covariate vector $\boldsymbol{x}$ includes as its components the variables of age group, gender, and pSES. We use $\boldsymbol{x} = (1, x_1, x_2, x_3, x_4)'$ where the age group indicator $x_1 = 1$ for the group of age 13–17 year-old, gender variable $x_2 = 1$ for male, and x_3 and x_4 are the dummy variables of the pSES variable with $x_3 = 1$ and $x_4 = 1$ for the second and third pSES categories, respectively. Here the baseline references for the three variables are age 0–12, female, and the first pSES category. Let $S(t; r)$ be the size of population of Albertans in sRHA r aged 0–18 at time t. The real population size at time t and region r is mostly unknown as it is only recorded for the sRHA level at the fiscal year end. For the purposes of this paper, we assume the population remains constant throughout the fiscal year. This assumption is not expected to have a large impact on the Poisson regression model when the population size is relatively large and the fluctuations throughout the year are expected to be minor.

Let $\psi(t)$ follow an autoregressive model of order 1 (i.e., AR(1)) and $\eta(r)$ be a spatial random effect. We use $R^{*,group}$ to denote the RHA R3, R6, R9 or the other RHAs. We consider the final model emerging from the discussions above and in Sections 2.2.1 and 2.2.2 below as follows:

$$\begin{aligned}\log\left\{\mathrm{E}\left[Y(t;r;\boldsymbol{x})\middle|\boldsymbol{x},\boldsymbol{b}(t,r),S(t,r)\right]\right\} = {} & \theta_0+\alpha_1(t,R^{*,group})x_1+\alpha_2(t,R^{*,group})x_2\\ & + \big(\alpha_3+b_3(r)\big)x_3+\big(\alpha_4+b_4(r)\big)x_4+\alpha_5\log S(t,r)+\big(\phi+b_\phi(r)\big)t\\ & + \big(A+b_A(r)\big)\cos\Big(\frac{2\pi t}{13}\Big)+\big(B+b_B(r)\big)\sin\Big(\frac{2\pi t}{13}\Big)+\beta_{12}x_1x_2+\beta_{13}x_1x_3\\ & + \beta_{14}x_1x_4+\omega_1x_3t+\omega_2x_4t+\psi(t)+\eta(r), \qquad (1)\end{aligned}$$

where θ_0 is the intercept, α_i, $i = 1, \ldots, 5$ are fixed effects and $b_3(r)$ and $b_4(r)$ are random effects of the demographic factors, and ϕ, A, and B are fixed seasonal effects and time trend, and $b_\phi(r)$, $b_A(r)$ and $b_B(r)$ are random seasonal effects and time trend. We will present further the structure of $\psi(t)$ and $\eta(r)$ in Section 2.2.2.

In the subsequent sections, we will explore the model and show evidence to justify the specific terms in Model (1). Model (1) is a special case of the following conventional generalized linear mixed effects model:

$$\begin{aligned}\log\left\{\mathrm{E}\left[Y(t,r,\boldsymbol{x})\middle|\boldsymbol{x},\boldsymbol{b}(t,r),S(t,r)\right]\right\} = {} & \boldsymbol{x}'\boldsymbol{\beta}(t,r)+\beta_5(t,r)\log S(t,r)\\ & + \beta_{12}x_1x_2+\beta_{13}x_1x_3+\beta_{14}x_1x_4+\beta_{23}x_2x_3\\ & + \beta_{24}x_2x_4+\omega_1x_3t+\omega_2x_4t+\psi(t)+\eta(r) \qquad (2)\end{aligned}$$

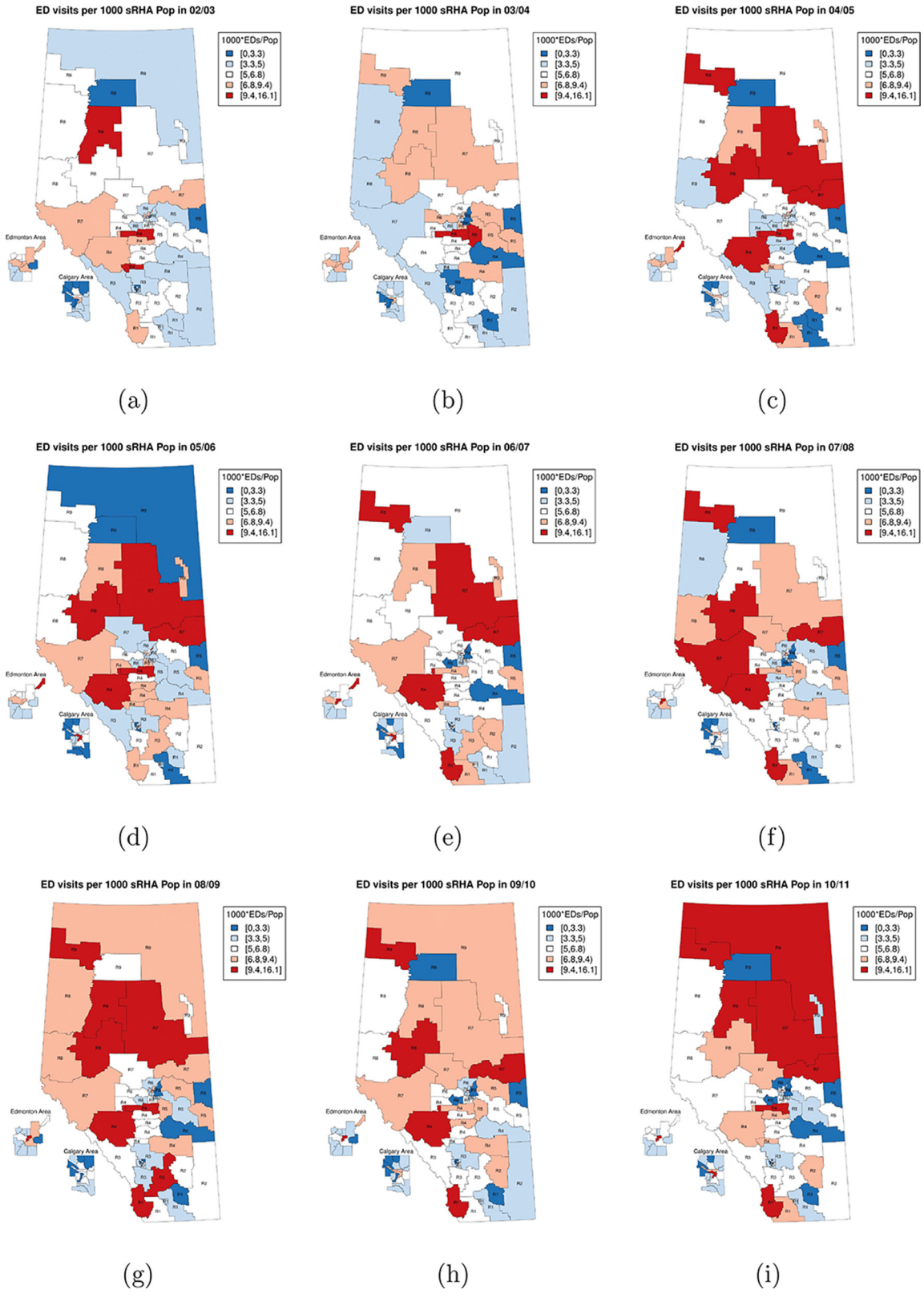

Fig. 1. MHED visits per 1000 sRHA in fiscal years: Fig. 1(a) 2002/2003; Fig. 1(b) 2003/2004; Fig. 1(c) 2004/2005; Fig. 1(d) 2005/2006; Fig. 1(e) 2006/2007; Fig. 1(f) 2007/2008; Fig. 1(g) 2008/2009; Fig. 1(h) 2009/2010, Fig. 1(i) 2010/2011.

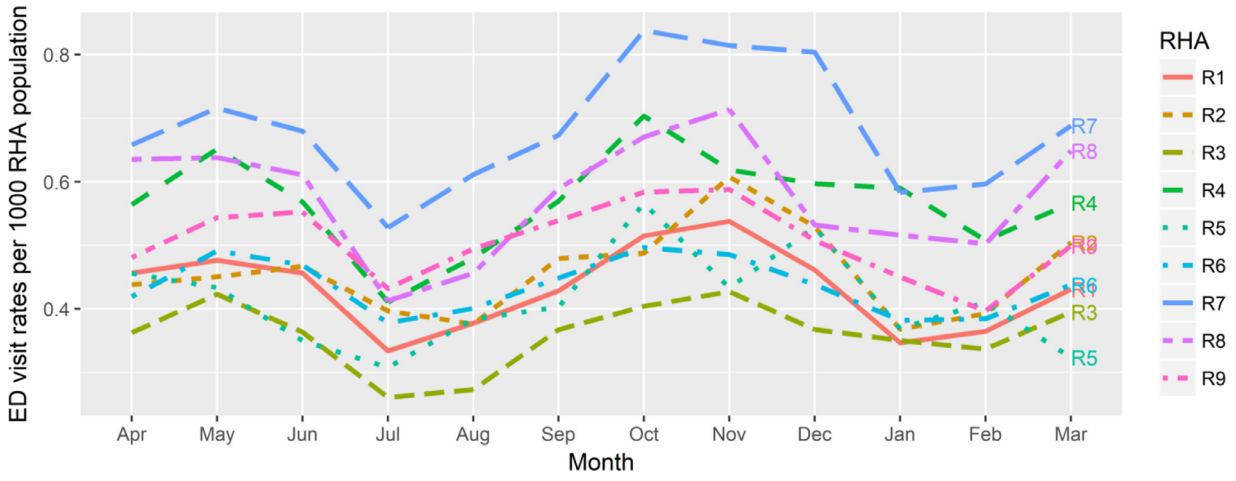

Fig. 2. Number of MHED visits per 1000 RHA population over monthly time aggregated over nine fiscal years.

with all the two-factor interactions assumed to be constant across time and space, and $\boldsymbol{\beta}(t,r) = (\beta_0(t,r), \beta_1(t,r), \beta_2(t,r), \beta_3(t,r), \beta_4(t,r))'$ to be

$$\beta_i(t,r) = \alpha_i(t,r) + b_i(t,r), \quad i = 0,\ldots,5,$$

where $\alpha_i(t,r)$, $i = 0,\ldots,5$ are fixed effects and the random effects $b_i(t,r)$, $i = 0,\ldots,5$ with $\boldsymbol{b}(t,r) = (b_0(t,r), b_1(t,r), b_2(t,r), b_3(t,r), b_4(t,r), b_5(t,r))' \sim MVN(0, \Sigma(t,r))$.

2.2.1. Fixed effects specifications

The fixed effect in the intercept $\alpha_0(t, r)$ can be expressed as $\alpha_0(t,r) = \theta_0(r) + h(t,r)$, where $h(t, r)$ describes the seasonal effect and time trend.

One may begin with considering the seasonal effect and time trend each of the regions: for region r^*,

$$h(t,r^*) = f_{trend,t}(t,r^*) + f_{seasonal,j(t)}(t,r^*),$$

where $j = 1,\ldots,13$ for the 13 blocks of size 28 days in a fiscal year and $t = 1,\ldots,117$ for the 13×9 time points, and $f_{trend,t}$ and $f_{seasonal,j(t)}$ are smoothing functions for the time trend and the cyclic seasonal pattern, respectively. The smoothing functions $f_{seasonal,j(t)}$ and $f_{trend,t}$ can be represented using a cyclic smoothing spline and thin plate smoothing spline, respectively. For example, the cyclic cubic spline is $f_{seasonal,j(t)} = \sum_{j=1}^{13-1} \tilde{b}_{j(t)}(j)\tau_{j(t)}$ with the basis functions $\tilde{b}_{j(t)}$. A characteristic of the cyclic cubic spline is that $f_{seasonal,1(t)}$ must match $f_{seasonal,13(t)}$ up to a second derivative (Wood, 2006).

We consider particularly the following two examples for the seasonal effect and time trend.

- Example T1. Assume a linear time trend and assign a coefficient for each of the $12 = 13 - 1$ blocks of size 28 days:

  $$h(t,r^*) = \phi(r^*)t + g_j(r^*),$$

  where $j = 1,\ldots,13$ for the 13 blocks of size 28 days in a year, and block 1 is the reference group $g_1 = 0$.
- Example T2. Assume a linear time trend and a seasonal pattern that is described by trigonometric functions:

  $$h(t,r^*) = \phi_0(r^*)t + A(t,r^*)\cos\left(\frac{2\pi t}{13}\right) + B(t,r^*)\sin\left(\frac{2\pi t}{13}\right).$$

The cyclic cubic smoothing spline for $f_{seasonal,j(t)}$ can be seen as an extension of Example T1: the spline smoothes over the discretized seasonal effect in the example. The thin plate spline may be used to check for whether a linear time trend is adequate or whether a polynomial time trend is required.

Fig. 3 shows the estimated time trend and the seasonal effect with the $13 - 1 = 12$ components in the model of Example T1, and with the trigonometric model of Example T2 for each RHA and the Alberta average. The seasonal patterns are similar in the models of Examples T1 and T2. To capture the seasonality in the MHED counts, the trigonometric model T2 is recommended over the cyclic cubic spline model and the $13 - 1$ factors for the blocks of size 28 days. This is due to the trigonometric model having fewer parameters compared to the seasonal factors model and trigonometric model being more interpretable compared to smoothing splines. The expressions $\cos(2\pi t/13) + \sin(2\pi t/13)$ account for the seasonal variation over time with the coefficients $A(t,$

Table 1
Number of MHED visits made by children/youth and number of children/youth with an MHED visit summarized by demographic information for each fiscal year.

	Fiscal Year								
	02/03	03/04	04/05	05/06	06/07	07/08	08/09	09/10	10/11
Total	4,278	4,258	4,472	4629	4,661	4,584	4,849	4,579	4,849
Gender									
Female	2,539	2,498	2,612	2,755	2,779	2,667	2,831	2,646	2,833
Male	1,739	1,760	1,860	1,874	1,882	1,917	2,018	1,933	2,016
Age									
0–5	56	62	51	43	53	64	58	70	40
6–12	437	365	441	478	494	446	467	411	479
13–18	3,785	3,831	3,980	4,108	4,114	4,074	4,324	4,098	4,330
pSES									
$pSES_1$	2,734	2,681	2,769	2,789	2,761	2,604	2,877	3,034	3,142
$pSES_2$	521	531	625	657	684	654	754	699	731
$pSES_3$	1,023	1,046	1,078	1,183	1,216	1,326	1,218	846	976

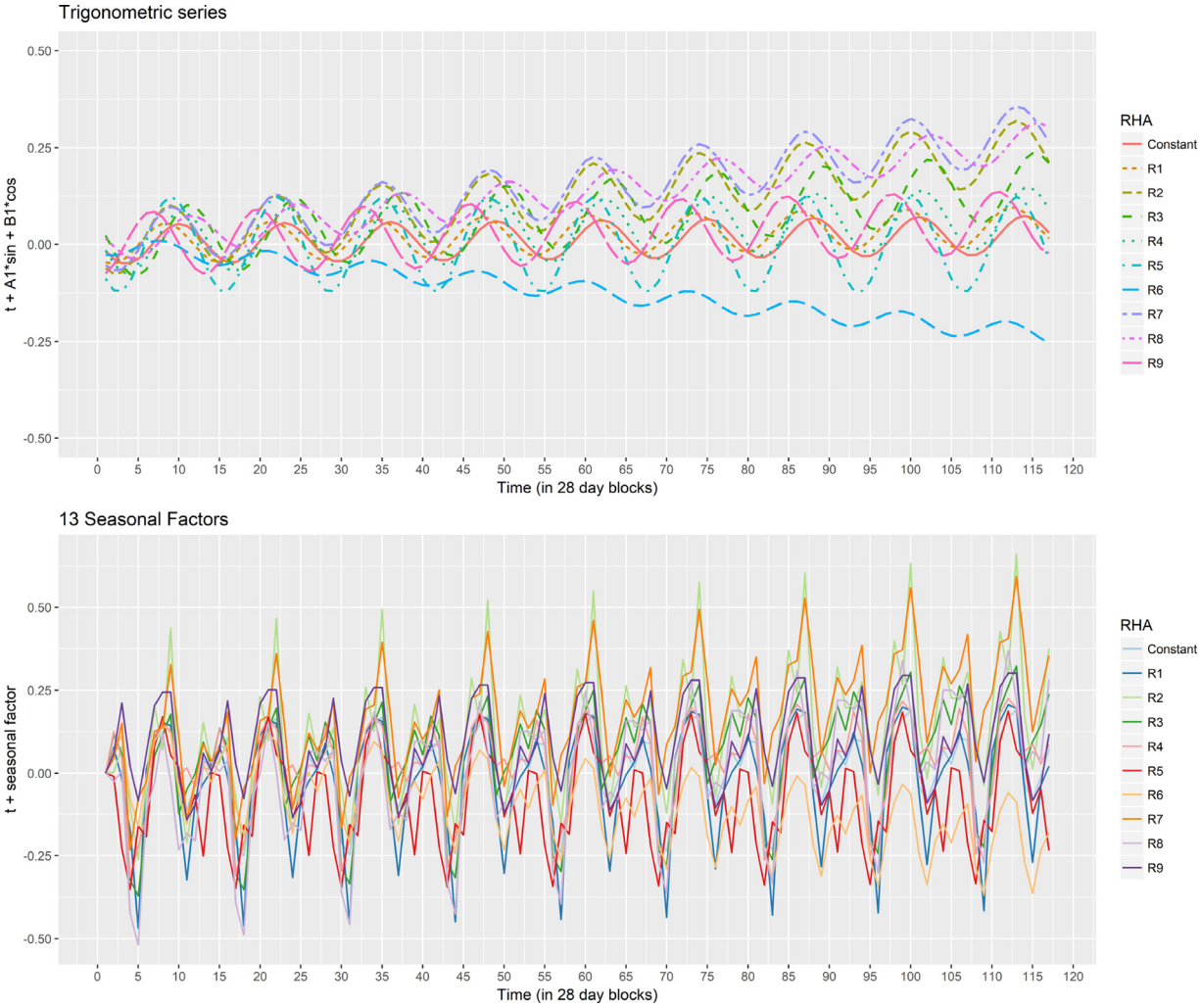

Fig. 3. Plots of the seasonal coefficients and time coefficient over the time unit (28 days) for Example T2 with trigonometric functions and Example T1 with 13 – 1 seasonal factors.

r^*) and $B(t, r^*)$ (Barnett and Dobson, 2010; Fanshawe et al., 2008; Torabi and Rosychuk, 2010).

To determine whether the coefficients should vary by region, the demographic, seasonal and time trend coefficients are proposed to be estimated under the following three different settings.

T1. Fix the coefficients to be constant.
T2. Allow the coefficients to vary by RHA.
T3. Allow the coefficients to vary by sRHA.

To achieve this, subsets of the data by RHA and sRHA for Settings T2 and T3 are fit to the models, respectively.

We compare first the coefficient estimates for the risk factors and exposures across the three different settings. In Fig. 4, we see the coefficients estimated by sRHA, RHA, and constant across all regions. The x-axis is the sRHA index and the y-axis is the coefficient's estimated value. The sRHA estimates of $\theta_0(r)$ and the log of the population coefficient fall inside the RHA or constant confidence interval (CI) estimates. The gender coefficient estimates by sRHA fall inside the constant CI estimate aside from sRHA R202 and sRHAs in RHAs R3 and R9. The gender coefficient estimates by sRHA all fall inside the RHA CI estimates. This motivates estimating the gender coefficient by RHA or groups of RHAs.

Fig. 5 shows that the teenage age group coefficient estimates vary by sRHA all fall inside the RHA CI estimate aside from R902. A large portion of the teenage coefficient estimates by sRHA in RHAs R3, R6, and R9 do not fall inside the constant CI estimate. Similar to the gender coefficient, the age group coefficient may be more informative if estimated by some grouping of the RHAs. Fig. 5 shows that none of the $pSES_2$ coefficient estimates varying by sRHA, compared to $pSES_1$, fall within the constant CI estimates. The sRHA coefficient estimates in RHA R5 fall inside the RHA CI estimate. For the $pSES_3$ coefficient estimates varying by sRHA, compared to $pSES_1$, the estimates for the Calgary area and Edmonton area RHAs R3 and R6, respectively, do not fall inside either the constant or RHA CI estimates. The majority of the estimates by sRHA in RHA R9 fall inside the constant and RHA CI estimates. The remaining estimates by sRHA fall inside their respective RHA CI estimate.

Our analysis indicates that the sRHAs belonging to the same RHA do not always follow the same pattern, particularly when looking at pSES. The sRHAs that tend to follow a different pattern from the overall average are from RHAs R3, R6 and R9. It is recommended the coefficients to be estimated under four groups: R3, R6, R9, and the remaining RHAs grouped into one category "Other".

To explore whether the coefficients to the risk factors vary across time, we estimate them in the following two settings.

Rt1. Assumes the coefficients for fixed effects α_i are constant across time and space; the time trend component of $h(t, r)$ is zero, and the seasonal effect is described by sine and cosine functions; there are no random effects.

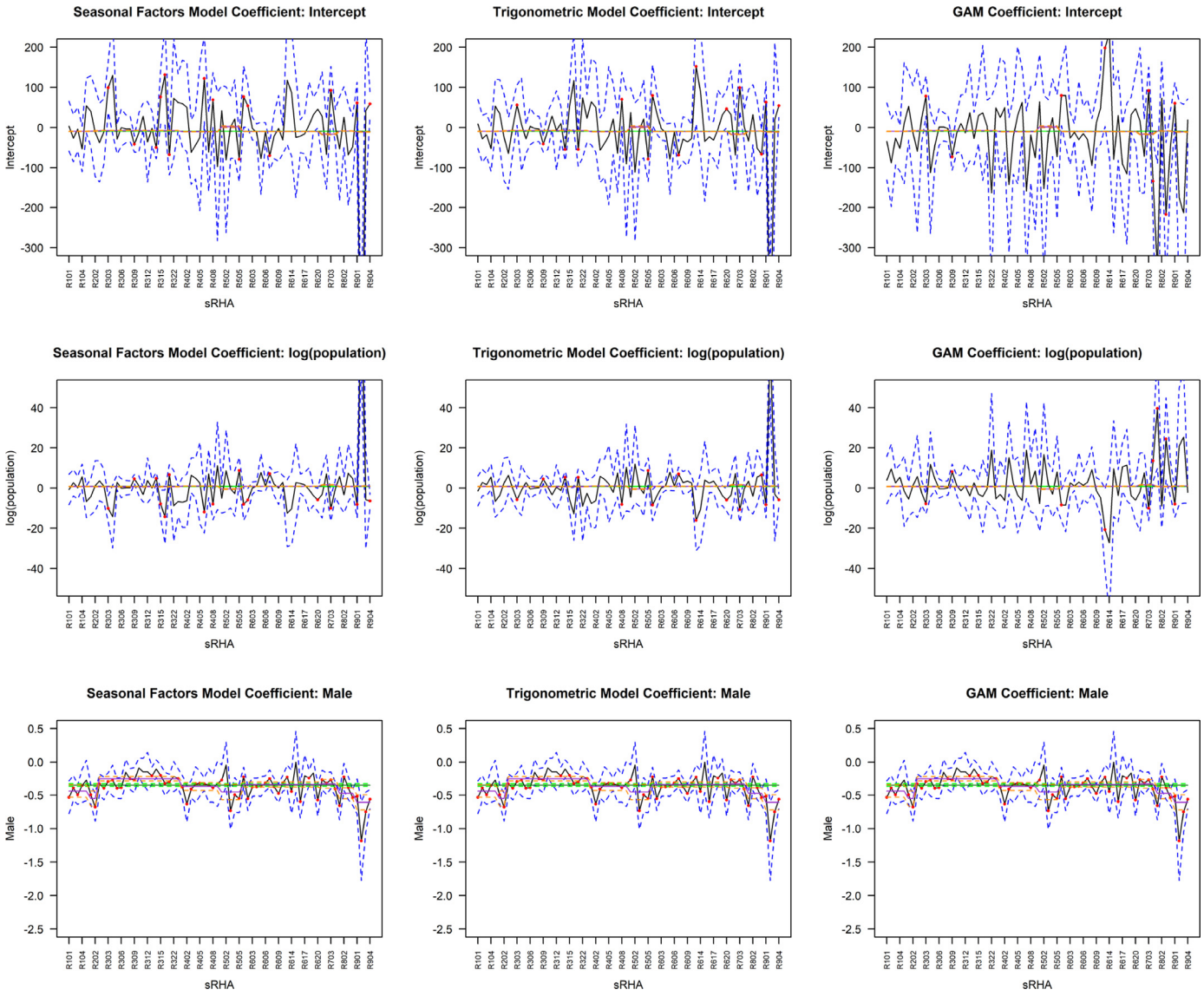

Fig. 4. Part I of the plots of the coefficient estimates for the seasonal factors (left), trigonometric (middle) and smoothing splines (right) models. The blue dotted lines are the 95% CI of the coefficients estimated by sRHA. The black line is the coefficient estimated by sRHA. The red points are the coefficient estimates significantly different from zero. The orange dashed lines are the 95% CI of the coefficients estimated by RHA. The purple line is the coefficient estimate by RHA. The green dashed lines are the 95% CI of the coefficient kept constant across regions.

Rt2. Assumes the fixed effects vary across time but are constant across space. To investigate how the seasonal effect varies over time, the fixed effects are assumed to vary across the nine fiscal years $t^*_{years} = 1, \ldots, 9$ rather than all $t = 1, \ldots, 117$ time points. Other assumptions are the same with Setting Rt1 above.

Table 2 summarizes the analysis results. Aside from fiscal year 2003/04, all of the estimates for the seasonal effect, A and B, fall inside the constant estimate's CI. For the coefficients for male and teenagers, all of the estimates fall within the constant CI estimates. This means the coefficients for the trigonometric seasonal effect, gender and age do not experience significant variation over yearly time. For the log of the population coefficient, fiscal years 2003/04 and 2008/09 do not fall within the constant CI estimates. Since the deviation from the constant CI estimates is small, less than 0.08, the constant estimate is recommended for log of the population in favour of a sparser model. For the pSES categories $pSES_2$ and $pSES_3$, fiscal years 2002/03, 2007/08, 2009/10, and 2010/11 do not fall within the constant CI estimates. This provides motivation for including an interaction term of time and pSES.

2.2.2. Random effects specifications

Fig. 3 indicates that the seasonality and time trend vary across the RHAs. Therefore, we include the random effects for the seasonal and time trend slopes in the model. An AR(1) model and a spatial random effect are considered to capture the temporal correlation and the correlation of regions, respectively. The random effect in the intercept $b_0(t; r)$ is assumed to include an AR(1) model based random effect, a spatial random effect, and random effects for the seasonal and time trend slopes:

$$b_0(t, r) = \psi(t) + \eta(r) + b_\phi(r)t + b_A(r)\cos\left(\frac{2\pi t}{13}\right) + b_B(r)\sin\left(\frac{2\pi t}{13}\right),$$

where $\psi(t)$ follows an AR(1) model, $\eta(r)$ is a spatial random effect component and $b_A(r)$, $b_B(r)$, and $b_\phi(r)$ are the random slopes varying by sRHA.

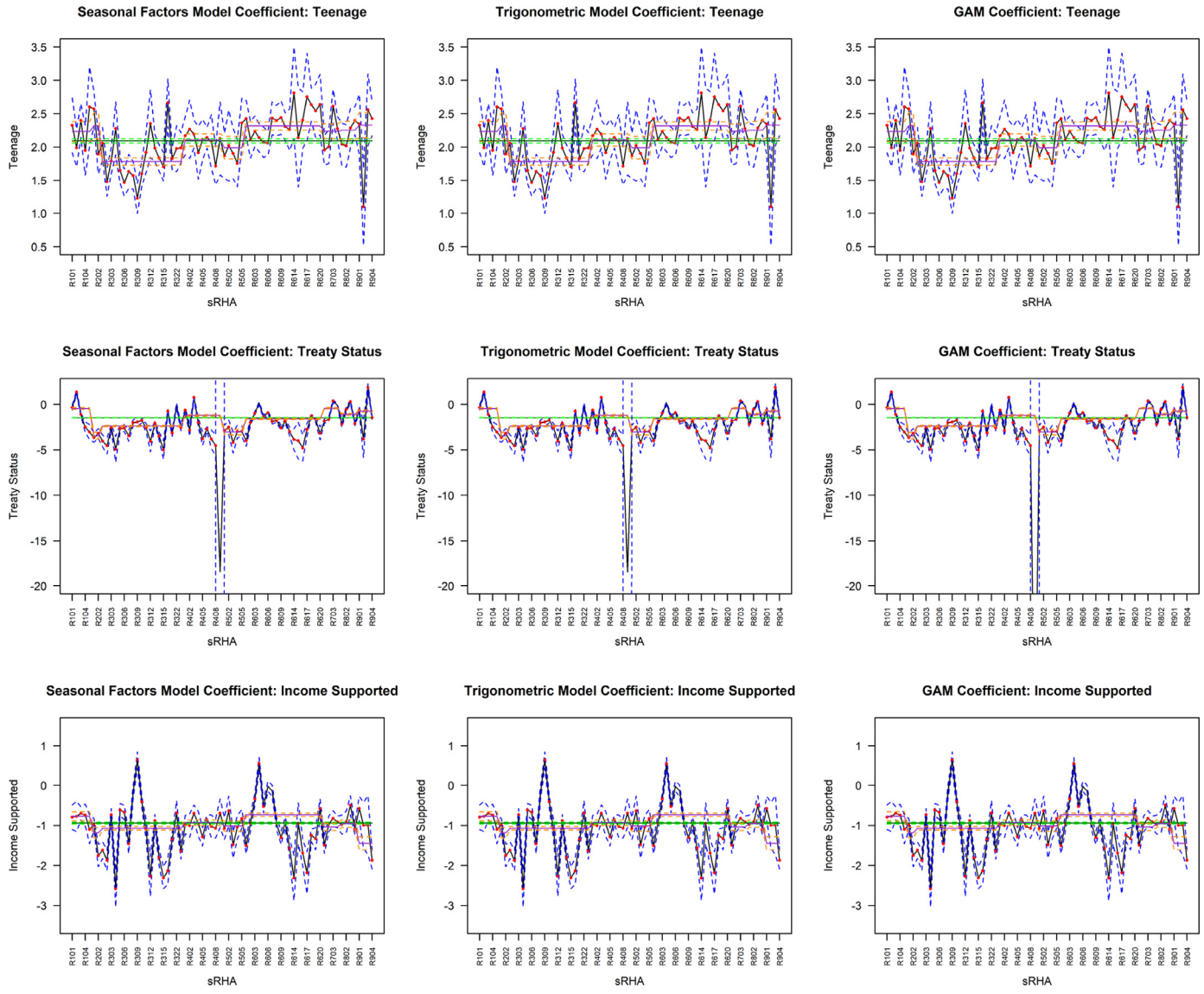

Fig. 5. Part II of the plots of the coefficient estimates for the seasonal factors (left), trigonometric (middle) and smoothing splines (right) models. The blue dotted lines are the 95% CI of the coefficients estimated by sRHA. The black line is the coefficient estimated by sRHA. The red points are the coefficient estimates significantly different from zero. The orange dashed lines are the 95% CI of the coefficients estimated by RHA. The purple line is the coefficient estimate by RHA. The green dashed lines are the 95% CI of the coefficient kept constant across regions.

Fig. 5 shows that the coefficient estimates for pSES have a large amount of variation between regions. This motivates the inclusion of a random slope for pSES that varies by the sRHA, $\beta_3(r) = \alpha_3 + b_3(r)$ and $\beta_4(r) = \alpha_4 + b_4(r)$. Denote $\widetilde{\boldsymbol{b}}(r) = (b_\phi(r), b_A(r), b_B(r), b_3(r), b_4(r))'$ with $\widetilde{\boldsymbol{b}}(r) \sim MVN(0, \Sigma_1)$. Following Waller et al. (1997), Martínez-Bereito et al. (2008), and Torabi and Rosychuk (2010), we assume that $\boldsymbol{\psi} = (\psi_1, \ldots, \psi_T) \sim N(\mathbf{0}, \boldsymbol{\Sigma}_\psi)$ with $\Sigma_\psi = \sigma_\psi^2/(1-\rho^2)\{\rho^{|t_1-t_2|}\}_{t_1,t_2=1}^{T}$. The parameter σ_ψ^2 is the temporal variance and ρ is the lag-1 temporal autocorrelation.

To explore different spatial correlation structures, three different versions of the spatial random effect $\eta(r)$ are considered:

S1. sRHA random effect: $\eta(r) = v(r)$ where $v(r) \sim N(0, \sigma_v^2)$.
S2. Hierarchical random effect: $\eta(r) = v(r) + u(R)$ where $v(r) \sim N(0, \sigma_v^2)$ and $u(R) \sim N(0, \sigma_u^2)$.
S3. CAR model: $\boldsymbol{\eta} = (\eta_1, \ldots, \eta_{70}) \sim N(\mathbf{0}, \boldsymbol{\Sigma}_\eta)$ where $\boldsymbol{\Sigma}_\eta = \sigma_\eta^2(\mathbf{I}_{70} - \lambda_\eta \mathbf{W})^{-1}$.

The first spatial random effect model assumes that there is an unknown heterogeneity between sRHAs. This is commonly referred to as a random intercept model (Agresti, 2013). The second model assumes that sRHAs within the same RHA are correlated. This model focuses on spatial correlation based on the geographic hierarchical structure created by the government of Alberta. Such a model is commonly referred to as a hierarchical or nested random effects model (Agresti, 2013). The third model is a CAR model, assuming adjacent sRHAs are correlated. In the proposed CAR model, σ_η^2 is the spatial dispersion, the scalar parameter λ_η describes the strength of spatial dependence among the observations (LeSage and Pace, 2009), $0 \leq \lambda_\eta < 1$, and $\mathbf{W}$ is the spatial weights matrix (Oliveira, 2012; Ver Hoef et al., 2018). The spatial weights matrix can be defined in various ways. One common definition is the adjacency matrix where if two different regions are adjacent, the corresponding matrix element will be 1 and 0 otherwise. We use this definition in the analysis.

The results from the model exploration showed there was evidence of variation over time and/or space for certain covariates.

Table 2
Summary of the coefficient estimates (± margin of error) with a trigonometric seasonal effect.

	Variable						
Estimate	log(S(t;r))	*A*	*B*	Male	Teen	$pSES_2$	$pSES_3$
Constant	0.82(± 0.02)	−0.01(±0.01)	−0.05(±0.01)	−0.35(±0.02)	2.09(± 0.03)	−1.47(±0.03)	−0.94(±0.04)
2002/03	0.88(± 0.06)	0.02(± 0.04)	−0.06(±0.04)	−0.38(±0.06)	2.04(± 0.10)	−1.66(±0.10)	−0.98(±0.07)
2003/04	0.92(± 0.06)	0.06(± 0.04)	−0.08(±0.04)	−0.35(±0.06)	2.19(± 0.10)	−1.62(±0.10)	−0.94(±0.07)
2004/05	0.85(± 0.05)	−0.05(±0.04)	−0.07(±0.04)	−0.34(±0.06)	2.09(± 0.10)	−1.49(±0.09)	−0.94(±0.07)
2005/06	0.84(± 0.05)	−0.02(±0.04)	−0.07(±0.04)	−0.39(±0.06)	2.07(± 0.09)	−1.45(±0.09)	−0.86(±0.07)
2006/07	0.75(± 0.05)	0.03(± 0.04)	−0.01(±0.04)	−0.39(±0.06)	2.02(± 0.09)	−1.39(±0.09)	−0.82(±0.07)
2007/08	0.83(± 0.05)	0.02(± 0.04)	−0.03(±0.04)	−0.33(±0.06)	2.08(± 0.09)	−1.38(±0.09)	−0.67(±0.07)
2008/09	0.74(± 0.05)	−0.05(±0.04)	−0.06(±0.04)	−0.34(±0.06)	2.11(± 0.09)	−1.34(±0.08)	−0.86(±0.07)
2009/10	0.76(± 0.05)	0.01(± 0.04)	−0.02(±0.04)	−0.31(±0.06)	2.14(± 0.10)	−1.47(±0.08)	−1.27(±0.08)
2010/11	0.81(± 0.05)	0.04(± 0.04)	−0.07(±0.04)	−0.34(±0.06)	2.12(± 0.09)	−1.46(±0.08)	−1.17(±0.07)

For the interaction with time, pSES was the only risk factor whose effect exhibited variation over time. The interaction term for gender and pSES was not found to be significant so it is excluded from the proposed models. Based on the preceding analysis, Model (1) is chosen as the final model.

3. Analysis procedure and results

3.1. Method of estimation

We conduct the data analysis by the R package INLA, which implements an integrated nested Laplace approximation (Rue et al., 2009) to approximate Bayesian analysis under the latent Gaussian models (LGMs), a subclass of structured additive regression models. An LGM consists of three elements: a likelihood model, a latent Gaussian field, and a vector of hyperparameters. The response variable Y is assumed to follow one of the exponential family distribution with mean μ. The mean is linked to a linear combination of the predictor through a known link function. The linear predictor is then additive with respect to a fixed term on the covariates plus random effects. The family of generalized linear mixed models (GLMMs) is an important subclass of LGMs with Gaussian priors on fixed and random effects (Breslow and Clayton, 1993; McCulloch et al., 2008). The use of INLA for Bayesian inference for GLMMs was investigated by Fong et al. (2010), who reanalyzed all of the examples from Breslow and Clayton (1993).

We carefully selected priors of the parameters of the random effects, the hyperparameters. The parameter estimates can be sensitive to the chosen priors (Rue et al., 2009). To let the data speak for itself, we set the priors of the parameters in the models of the random effects to be highly vague and likely plausible. The prior distributions for the parameters in the AR(1) model and in the CAR model are chosen to be

$$\log\left(\frac{1+\rho}{1-\rho}\right) \sim N(0, 0.15) \text{ and } -\log(\sigma_\psi^2/(1-\rho^2)) \sim \log \text{ Gamma}(1, 0.0001),$$

and

$$-\log(\sigma_\eta^2) \sim \log \text{ Gamma}(1, 0.0001) \text{ and } \log\left(\frac{\lambda_\eta}{1-\lambda_\eta}\right) \sim N(0, 10).$$

The prior for ρ is kept at the recommended default prior in INLA. The prior for λ_η is set to be a more vague prior compared to ρ due to the posterior distribution of λ_η being unstable and multimodal at the default $N(0, 0.1)$ recommended by INLA. In INLA, $\boldsymbol{\Sigma_\eta}$ is specified as

$$\boldsymbol{\Sigma_\eta} = \sigma_\eta^2\left(\boldsymbol{I} - \frac{\lambda_\eta}{\max \text{ eigenvalue of } W}\boldsymbol{W}\right)^{-1},$$

to ensure λ_η is in the range [0, 1). The prior distributions for the random seasonal slope, time trend slope, pSES slope, and nested sRHA within RHA effects are set to be the same highly vague distribution. That is, we have $-\log(\sigma^2) \sim \log \text{ Gamma}(1, 0.0001)$, where σ^2 corresponds to the random seasonal slope, time trend slope, pSES slope, RHA intercept, or sRHA intercept variance parameter.

Table 3
WAIC and DICs for three different spatial random effects specifications.

Random effect $\eta(r)$	DIC	Eff. parameters	WAIC	Eff. parameters
1. sRHA	119,645	484	119,561	407
2. Hierarchical	119,646	483	119,562	407
3. CAR	119,646	484	119,562	407

3.2. Analysis results

3.2.1. Spatial correlation structure

Three different spatial random effects models are proposed to describe the correlation among sRHAs. The first assumed independence in sRHAs, the second assumed sRHAs within the same RHA are correlated and the third assumed adjacent sRHAs are correlated. To assess whether the model fit improves with the inclusion of different spatial random effects, the deviance information criteria (DIC) and Watanabe-Akaike information criteria (WAIC) are used. A lower DIC and WAIC compared to other nested models means the model is a better fit. The WAIC and DIC of the three proposed models are displayed in Table 3. There is no discernible difference between the three models' information criterions. The estimated covariance between sRHAs in the same RHA and the estimated covariance between adjacent sRHAs is small, approximately 0.01. The model could include either a CAR model, nested random effects, or a random effect for the sRHA since there is a negligible difference between their information criterions and the number of effective parameters. The first model, the sRHA random effect model, is chosen in favour of a simpler model.

3.2.2. Final model specification

The 95% CI for the log of the population size coefficient, α_5, contained 1 so it is treated as an offset term in the model. Initially, the random slopes of the seasonal, time trend, and pSES with sRHA random effects were assumed to be correlated. The 95% CIs of these correlation estimates all contained 0 and contributed no improvement to the model fit so the random effects are assumed to be independent of each other, $b_\phi(r) \sim N(0, \sigma_\phi^2)$, $b_A(r) \sim N(0, \sigma_A^2)$, $b_B(r) \sim N(0, \sigma_B^2)$, $b_3(r) \sim N(0, \sigma_{b_3}^2)$, and $b_4(r) \sim N(0, \sigma_{b_4}^2)$. The estimates of this model use a scaled t, where $t = 1, \ldots, 117$ is scaled to range from (0,1] by dividing t by its maximum index, 117. This ensures the parameter estimates are on a similar scale where the categorical risk factors are binary with value 0 or 1 and the trigonometric functions sine and cosine range from $[-1, 1]$.

Table 4
Summary of final model estimates with scaled t and AR(1), sRHA, pSES, seasonal and time trend random effects.

Variable	Mean	95% CI
θ_0	−11.579	(−11.702, −11.457)
A	0.013	(−0.035, 0.062)
B	−0.051	(−0.101, −0.001)
ϕ	0.024	(−0.120, 0.167)
Male and R3	0.584	(0.517, 0.650)
Male and R6	0.539	(0.471, 0.608)
Male and R9	0.259	(0.133, 0.383)
Male and Other RHAs	0.467	(0.401, 0.533)
Teenage and R3	2.383	(2.315, 2.451)
Teenage and R6	2.883	(2.807, 2.961)
Teenage and R9	2.683	(2.513, 2.858)
Teenage and Other RHAs	2.712	(2.643, 2.781)
$pSES_2$	−2.687	(−3.069, −2.310)
$pSES_3$	−0.671	(−0.830, −0.511)
$pSES_2$ × t	0.307	(0.199, 0.415)
$pSES_3$ × t	−0.150	(−0.232, −0.067)
$pSES_2$ × Teenage	0.274	(0.169, 0.380)
$pSES_3$ × Teenage	−0.357	(−0.427, −0.287)
Male × Teenage	−0.977	(−1.041, −0.913)
σ^2_ν	0.108	(0.076, 0.164)
σ^2_ψ	0.017	(0.013, 0.025)
ρ	0.375	(0.194, 0.556)
σ^2_A	0.001	(0.001, 0.004)
σ^2_B	0.003	(0.001, 0.006)
σ^2_ϕ	0.050	(0.031, 0.084)
$\sigma^2_{b_3}$	2.223	(1.610, 3.270)
$\sigma^2_{b_4}$	0.338	(0.246, 0.505)

3.2.3. Analysis results

The final model estimates are displayed in Table 4. As shown, the 95% CIs for A and ϕ contain 0, which means the seasonal and time trend fixed effect terms are not significant. These fixed effects will remain in the model as the means of their random effects. Interaction of gender and age shows male children have more MHED visits compared to female children but female teenagers have more MHED visits compared to male teenagers. The interaction between time and pSES show that the $pSES_2$ group experiences an upward trend in MHED visits, but the $pSES_3$ group experiences a downward trend. The estimates of the random effect parameter for the temporal, σ^2_ψ, is small, but the temporal autocorrelation estimate, ρ, is fairly large. The variance estimates for the seasonal and time trend random slopes are quite small. These slopes could be small due to the AR(1) model random effect capturing the majority of the variation due to time. The variance estimates for $b_3(r)$ and $b_4(r)$ are fairly large, which means pSES had a large amount of variation across regions.

We explored the over-dispersion issue with the MHED counts. In initial analysis when we did not include the random effect components, we checked the count data for over-dispersion. The dispersion parameter was always estimated to be less than 2. In addition,the standard errors under the negative binomial model did not differ much from the ones under the Poisson model. We observed that the goodness of fit the negative binomial model was not better than the one with the Poisson model. The results of the probability integral transform histogram also indicate that the MHED counts are not noticeably over-dispersed. This is verified by the non U-shaped histogram of the PIT values in Fig. 6.

3.3. Predictive accuracy measures

To check the model fit and whether there are any outliers, the conditional predictive ordinates (CPO) and probability integral transform (PIT) values can be examined. The CPO and PIT are defined as

$$\text{CPO}_i = \pi(y_i^{\text{obs}}|\boldsymbol{y}_{-i}) \quad \text{and} \quad \text{PIT}_i = \text{Prob}(y_i^{\text{new}} \le y_i|\boldsymbol{y}_{-i}). \tag{3}$$

Since our response is discrete, the PIT values are modified to: $\text{PIT}_i^* = \text{PIT}_i - 0.5\,\text{CPO}_i$. The CPO is determined through leave-one-out cross-validation (Rue et al., 2009) and it expresses the posterior probability of observing y_i when the model is fitted to all the data except y_i. Small CPO values suggest that y_i is an outlier and higher values implies a better model fit. A CPO value is considered small when its inverse is greater than 40 and an extreme value when its inverse is greater than 70 (Ntzoufras, 2009). From Fig. 6, the plots of the CPO values indicate there are some outliers however the amount is relatively small. The small CPO values account for approximately 2% of the data points. The histogram of the CPO values shows that the majority of the values are large.

The PIT values are also determined through leave-one-out cross-validation (Rue et al., 2009). For the modified PIT values, if their histogram does not look like a uniform distribution then there may be issues with the model specification. A U-shaped histogram indicates under-dispersed predictive distributions, an inverse U-shaped histogram indicates over-dispersion and a skewed histogram indicates the central tendencies are biased (Czado et al., 2009). The PIT values in Fig. 6 are skewed to the left. This indicates that our model tends to have fitted values smaller than the true observations. This could be due to a variety of reasons such as unexplained variation due to variables not included in the model or due to the outliers the CPO values found. Fig. 7 shows the fitted MHED visits per 1000 sRHA population of the subgroup females aged greater than 12. We see from the plots that the model has difficulty fitting the large MHED rates, like we saw with the PIT values, but the model captures the overall rate.

4. Discussion

This paper explores the spatio-temporal patterns of MHED visits made by children and adolescents in Alberta. To capture the time trend and the seasonal patterns of the data, a smoothing spline model, a seasonal factors model, and a trigonometric model are proposed. To observe the differences among regions and over time, the coefficients are allowed to vary over time and space. A generalized linear mixed model is proposed and age, gender, and the proxy for socio-economic status are found to be important risk factors associated with MHED visits. We observe that male children have more MHED visits compared to female children but female teenagers have more MHED visits compared to male teenagers. The effect of pSES varies over time but the seasonal effects and the remaining risk factors do not. Effects of the risk factors associated with RHAs 3, 6, and 9 differ from the other RHAs.

Multiple papers have examined the frequency, demographic characteristics, and usage of EDs for mental health reasons among children and youth; recent examples include Mapelli et al. (2015), Kalb et al. (2019), Tran et al. (2019), Ruzangi et al. (2020), and Lo et al. (2020). However, there is a paucity of literature on the spatial or spatio-temporal modeling of ED visits. Using the same data extract as the current study, space and time clustering analyses of adolescents aged 10 to 17 with ED visits for mood disorders (Rosychuk et al., 2014), of adolescents aged 15 to 17 with ED visits for self-harm (Rosychuk et al., 2016), and of adolescents aged 15 to 17 presenting with mental or behavioral disorder secondary to alcohol and other drug use (Newton et al., 2016) have been conducted. Analyses were adjusted by sex or sex and age group and all analyses identified clusters in the northern region of the province and various other clusters depending on the health condition examined. Those analyses were more limited than our study as they did not model spatial and temporal trends in the data using generalized linear mixed models that capture time trends and seasonal patterns with predictor variables. There are few spatial modeling studies of ED visits to offer any direct comparisons with our study. Spatial temporal hurdle models have been used to

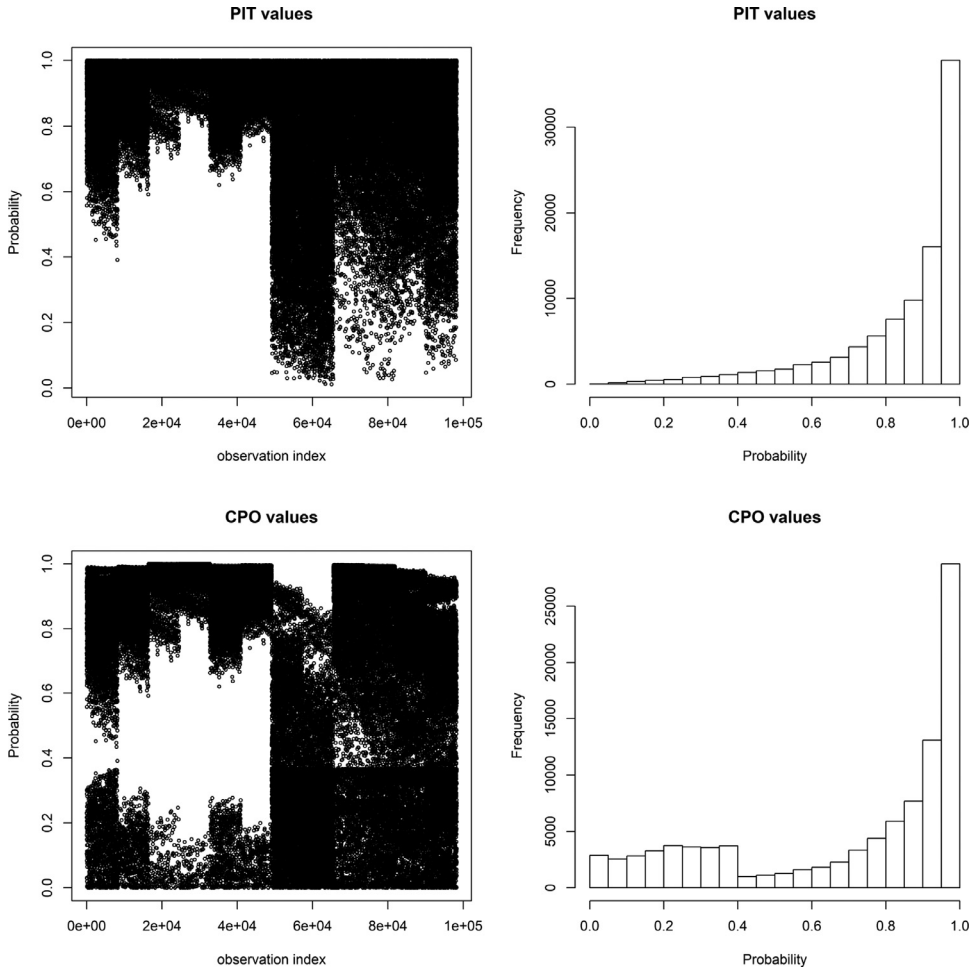

Fig. 6. CPO and PIT values for proposed model.

assess the effect of patient- and region-level predictors like age, sex, race, insurance, and poverty level on ED use in Durham County census blocks in North Carolina during 2007–2011 (Neelon et al., 2016; 2013). These studies included children and adults and did not consider particular diagnoses like mental health. In Manchester, England, ED visits for self-harm during 2002–2013 made by subjects aged $\geq$ 10 years were analyzed using Bayesian hierarchical models and Moran's I was also used to identify clustering in local areas (Lin et al., 2019). During 2005–2014 for eight counties in New York state,Zhang et al. (2020) looked at ED visits for patients of any age for several health conditions, including mental disorders, with an emphasis on comparing the time period of Superstorm Sandy with the same period in other years. The authors considered spatial clustering to group census tracts and developed nonlinear models to evaluate health risk and develop a community vulnerability index. These study results are not directly comparable to our study given that the jurisdictions, age group, diagnosis, and methodological approaches vary considerably.

Overall, spatio-temporal patterns in MHED use is evidenced by our analysis, and our model helps to identify important demographic factors from gender, age, and socio-economic status. The analysis reveals that some demographic groups are more susceptible to experience MHED visits than the other groups. A variety of issues need to be addressed to further enhance the value of this research.

Our model assumes lag-1 temporal autocorrelation. The estimate of ρ is found to be significant from zero. A larger lag might show significant temporal autocorrelation for time points further apart. The analysis outcomes show that sRHAs in the same RHA and adjacent sRHAs are not significantly correlated. This suggests that the hierarchical structure of sRHAs in RHAs is not very strong. The spatial weights matrix considered in this paper is based on the adjacency of two regions, which is based on the Cliff and Ord (1973) spatial autocorrelation definition. Different forms of spatial contiguity could be considered, such as distance thresholds. Distance-based spatial contiguity may yield different results.

As pointed out by Rue et al. (2009), the parameter estimates can be sensitive to the chosen priors. To explore the effect of the prior distribution on the model and parameter estimates, we assign weakly informative prior distributions to the variance parameters. The prior distributions for ρ and λ_η remain the same but the remaining parameters are set such that $-\log(\sigma^2) \sim \log \text{Gamma}(0.1, 0.1)$. The parameter estimates with weakly informative prior distributions are similar aside from the estimate for the RHA random effect and the random slope for the time trend grouped by region. The highly vague prior distributions estimated these effects to be very small but the weakly informative prior distributions estimated them to be larger due to a stricter distribution setting. Despite the differences in these parameter estimates, the information criterions remain largely the same.

Moreover, individuals in this data can have multiple MHED visits which makes the data recurrent event data, meaning that MHED visits made by the same individual are correlated. This paper focuses on aggregate-level data but future investigations could incorporate this correlation structure by considering individual-level data. In addition, the spatial and temporal effects are

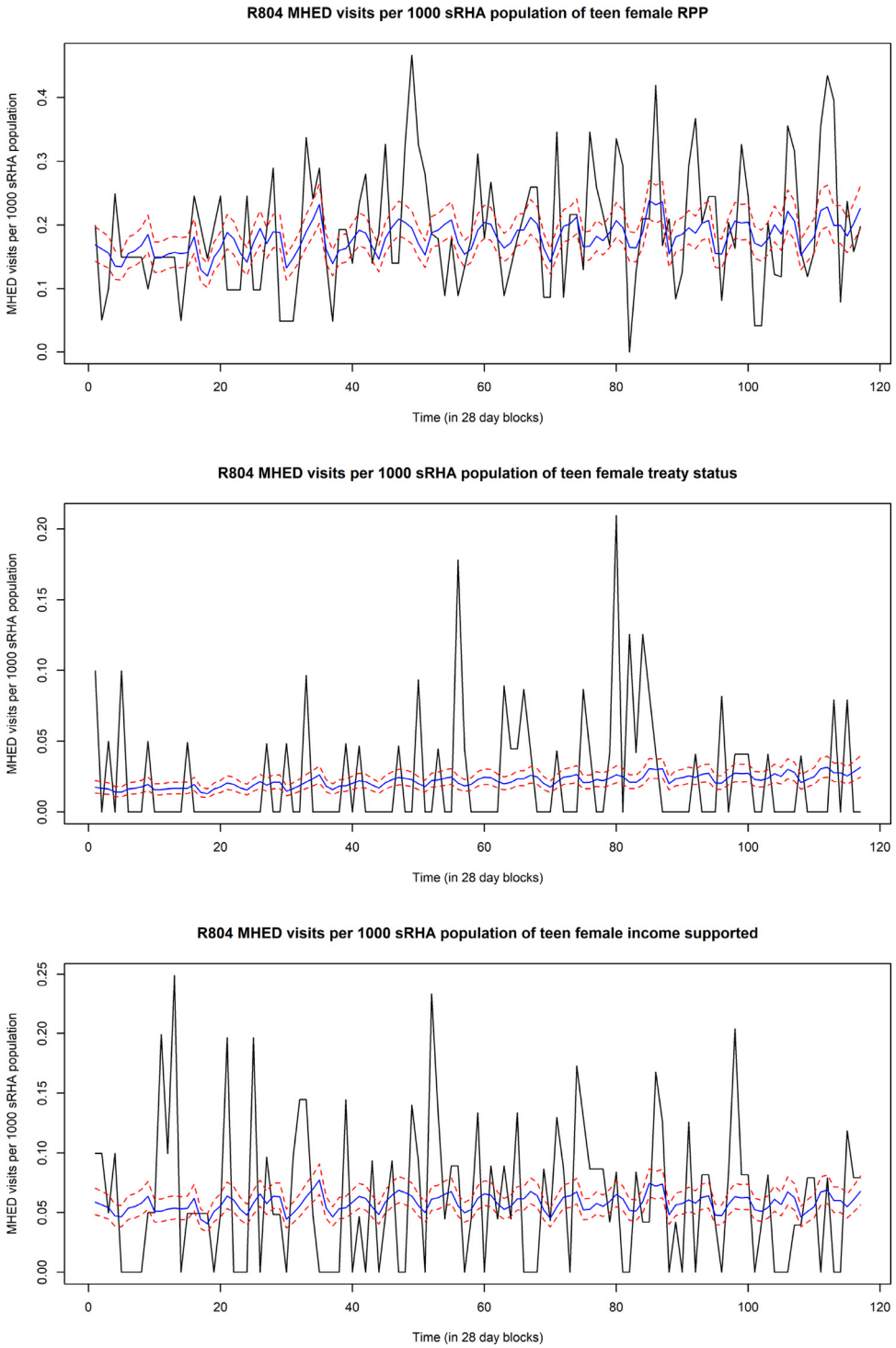

Fig. 7. Plots of true and fitted MHED visits per 1000 sRHA population for females aged greater than 12 in sRHA R804 with socio-economic status $pSES_1$, $pSES_2$ or $pSES_3$. The black line is the true rates, the blue line is the fitted posterior means and the dashed red lines are the 2.5% and 97.5% quantiles of the fitted posterior mean.

considered separately in the model. A more informative model might include an interaction term for space and time. This can be implemented through a random effect that takes the Kronecker product of a temporal and spatial structure matrix, such as the AR(1) and CAR structure (Clayton, 1996).

We remark that there are limitations with the PMHC dataset. First, the population count information is incomplete since it is only available at the fiscal year end. Interpolation could be used to estimate the population counts in between years. Second, the records of the MHED visits were from individuals less than 18 years of age during April 1, 2002, to March 31, 2011, which gives rise to doubly censored data. Third, the smallest unit for the spatial information regarding the subject's place of residence is only available at the sRHA level. The spatial information is unavailable as point data, but rather polygon data, so there is a loss of information. Fourth, the presence of other mental health services in the region can be a potential confounder. Some regions could have fewer MHED visits due to access to other mental health services.

However, the PMHC dataset does not contain information on whether individuals visited other mental health services.

Future investigations plan on including information such as the patient's triage level and diagnosis. Triage level gives an indication of the severity of the child or youth's MHED visit. Lastly, knowing which sRHAs are expected to experience large amounts of MHED visits given their population size, and at what time period to expect these MHED visits could be helpful to the government of Alberta. In the future, we plan on investigating the predictive abilities of our model.

Declaration of Competing Interest

None.

Disclaimer

This article is based in part on data provided by Alberta Health. The interpretation and conclusions are contained herein are those of the researchers and do not necessarily represent the views of the Government of Alberta. Neither the government nor Alberta Health expresses any opinion in relation to this study.

CRediT authorship contribution statement

Michelle Thiessen: Conceptualization, Formal analysis, Investigation, Methodology, Software, Validation, Visualization, Writing - original draft. **Qi Cui:** Investigation, Validation, Visualization, Writing - original draft, Writing - review & editing. **X. Joan Hu:** Conceptualization, Funding acquisition, Methodology, Project administration, Supervision, Writing - original draft, Writing - review & editing. **Rhonda J. Rosychuk:** Data curation, Funding acquisition, Methodology, Project administration, Supervision, Writing - review & editing.

Funding

This research is supported by research grants to XJH and RJR from the Canadian Institutes of Health Research (CIHR) and the Natural Sciences and Engineering Research Council of Canada (NSERC). The sponsors had no role in the study design, in the collection, analysis and interpretation of data, in the writing of the report, and in the decision to submit the article for publication.

Acknowledgements

The authors thank Alberta Health for facilitating access to the data.

References

Agresti, A., 2013. Categorical Data Analysis, third ed. Wiley Series in Probability and Statistics.
Barnett, A.G., Dobson, A.J., 2010. Analysing Seasonal Health Data. Springer.
Breslow, N.E., Clayton, D.G., 1993. Approximate inference in generalized linear mixed models. J. Am. Stat. Assoc. 88 (421), 9–25.
Clayton, D.G., 1996. Generalized linear mixed models. In: Gilks, R., Richardson, S., Spiegelhalter, D.J. (Eds.), Markov Chain Monte Carlo in Practice. Chapman and Hall, London, pp. 275–301.
Cliff, A.D., Ord, J.K., 1973. Spatial Autocorrelation. Pion.
Czado, C., Gneiting, T., Held, L., 2009. Predictive model assessment for count data. Biometrics 65 (4), 1254–1261.
Fanshawe, T.R., Diggle, P.J., Rushton, S., Sanderson, R., Lurz, P.W.W., Glinianaia, S.V., Pearce, M.S., Parker, L., Charlton, M., Pless-Mulloli, T., 2008. Modelling spatio-temporal variation in exposure to particulate matter: a two-stage approach. Environmetrics 19, 549–566.
Fong, Y., Rue, H., Wakefield, J., 2010. Bayesian inference for generalized linear mixed model. Biostatistics 11 (3), 397–412.
Hu, X.J., Rosychuk, R.J., 2016. Marginal regression analysis of recurrent events with coarsened censoring times. Biometrics 72, 1113–1122.
Jenks, G.F., 1977. Optimal Data Classification for Choropleth Maps. Technical Report. Department of Geography, University of Kansas, Lawrence.
Kalb, L.G., Stapp, E.K., Ballard, E.D., Holingue, C., Keefer, A., Riley, A., 2019. Trends in psychiatric emergency department visits among youth and young adults in the us. Pediatrics 143 (4). doi:10.1542/peds.2018-2192.
Kulldorff, M., Nagarwalla, N., 1995. Spatial disease clusters: detection and inference. Stat. Med. 14 (8), 799–810.
Leitch, K.K., 2007. Reaching for the Top: A Report by the Advisor on Healthy Children and Youth. Health Canada, Ottawa, ON.
LeSage, J., Pace, R.K., 2009. Introduction to Spatial Econometrics. CRC Press.
Lin, C.Y., Bickley, H., Clements, C., Webb, R.T., Gunnell, D., Hsu, C.-Y., Chang, S.-S., Kapur, N., 2019. Spatial patterning and correlates of self-harm in manchester, england. Epidemiol. Psychiatr. Sci. 29, e72.
Lo, C.B., Bridge, J.A., Shi, J., Ludwig, L., Stanley, R.M., 2020. Children's mental health emergency department visits: 2007–2016. Pediatrics 145 (6).
Mapelli, E., Black, T., Doan, Q., 2015. Trends in pediatric emergency department utilization for mental health-related visits. J. Pediatr. 167 (4), 905–910.
Mariathas, H.H., Rosychuk, R.J., 2015. An examination of three spatial event cluster detection methods. ISPRS Int. J. Geo-Inform. 4, 367–384.
Martínez-Bereito, M.A., López-Quilez, A., Botella-Rocamora, P., 2008. An autoregressive approach to spatio-temporal disease mapping. Stat. Med. 27, 2874–2889.
McCulloch, C.E., Searle, S.R., Neuhaus, J.M., 2008. Generalized, Linear, and Mixed models, second ed. John Wiley and Sons, New York.
Mental Health Commission of Canada, 2012. Changing directions, changing lives: the mental health strategy for Canada. Available at https://www.mentalhealthcommission.ca/sites/default/files/MHStrategy_Strategy_ENG.pdf.
Neelon, B., Chang, H.H., Ling, Q., Hastings, N.S., 2016. Spatiotemporal hurdle models for zero-inflated count data: exploring trends in emergency department visits. Stat. Methods Med. Res. 25 (6), 2558–2576.
Neelon, B., Ghosh, P., Loebs, P.F., 2013. A spatial poisson hurdle model for exploring geographic variation in emergency department visits. J. R. Stat. Soc. Ser. A 176 (2), 389–413.
Newton, A. S., Rosychuk, R. J., Ali, S., Cawthorpe, D., Curran, J., Dong, K., Slomp, M., Urichuk, L., 2011. The Emergency Department Compass: Children's Mental Health. Pediatric mental health emergencies in Alberta, Canada: Emergency department visits by children and youth aged 0 to 17 years, 2002–2008. Edmonton, AB.
Newton, A.S., Shave, K., Rosychuk, R.J., 2016. Does emergency department use for alcohol and other drug use cluster geographically? A population-based retrospective cohort study. Substance Use Misuse 51 (9), 1239–1244.
Ntzoufras, I., 2009. Bayesian Modeling Using WingBUGS. John Wiley and Sons.
Oliveira, V., 2012. Bayesian analysis of conditional autoregressive models. Ann. Inst. Stat.Math. 64 (1), 107–133.
Rosychuk, R.J., Johnson, D.W., Urichuk, L., Dong, K., Newton, A.S., 2016. Does emergency department use and post-visit physician care cluster geographically and temporally for adolescents who self-harm? A population-based 9-year retrospective cohort study from Alberta, Canada. BMC Psychiatry 16, 229.
Rosychuk, R.J., Newton, A.S., Hu, X.J., 2018. Age affects the impact of important predictors on mental health emergency department visits. J. Behav. Health Serv.Res. 1–11.
Rosychuk, R.J., Newton, A.S., Niu, X., Urichuk, L., 2014. Space and time clustering of adolescents' emergency department use and post-visit physician care for mood disorders in Alberta, Canada: a population-based 9-year retrospective study. Canadian J. Public Health 106 (2), 10–16.
Rue, H., Martino, S., Chopin, N., 2009. Approximate Bayesian inference for latent Gaussian models using integrated nested Laplace approximations (with discussion). J. R. Stat. Soc.Ser. B 71 (2), 319–392.
Ruzangi, J., Blair, M., Cecil, E., Greenfield, G., Bottle, A., Hargreaves, D.S., Saxena, S., 2020. Trends in healthcare use in children aged less than 15 years: a population-based cohort study in england from 2007 to 2017. BMJ Open 10 (5).
Torabi, M., Rosychuk, R.J., 2010. Spatio-termporal modelling of disease mapping of rates. Canadian J. Stat. 38 (4), 698–715.
Tran, Q.N., Lambeth, L.G., Sanderson, K., de Graaff, B., Breslin, M., Tran, V., Huckerby, E.J., Neil, A.L., 2019. Trends of emergency department presentations with a mental health diagnosis by age, australia, 200405 to 201617: a secondary data analysis. Emergency Med. Australasia 31 (6), 1064–1072.
Ver Hoef, J.M., Peterson, E.E., Hooten, M.B., Hanks, E.M., Fortin, M.J., 2018. Spatial autoregressive models for statistical inference from ecological data. Ecol. Monogr. 88 (1), 36–59.
Waller, L.A., Carlin, B.P., Xia, H., Gelfand, A.E., 1997. Hierarchical spatio-temporal mapping of disease rates. J. Am. Stat. Assoc. 92, 607–617.
Wood, S.N., 2006. Generalized Additive Models: An introduction with R. CRC Press.
Zhang, W., Kinney, P.L., Rich, D.Q., Sheridan, S.C., Romeiko, X.X., Dong, G., Stern, E.K., Du, Z., Xiao, J., Lawrence, W.R., Lin, Z., Hao, Y., Lin, S., 2020. How community vulnerability factors jointly affect multiple health outcomes after catastrophic storms. Environ. Int. 134, 105285.